CdS and $Cd(OH)_2$ formation during Cd treatments of $Cu(In,Ga)(S,Se)_2$ thin-film solar cell absorbers

L. Weinhardt, Th. Gleim, O. Fuchs, C. Heske,[a] and E. Umbach
Experimentelle Physik II, Universität Würzburg, Am Hubland, 97074 Würzburg, Germany

M. Bär, H.-J. Muffler, Ch.-H. Fischer, and M. C. Lux-Steiner
Department SE 2, Hahn-Meitner-Institut, Glienicker Straße 100, 14109 Berlin, Germany

Y. Zubavichus
Angewandte Physik Chemie, Universität Heidelberg, 69120 Heidelberg, Germany

T. P. Niesen and F. Karg
Shell Solar, D-81739 Munich, Germany

(Received 14 June 2002; accepted 26 November 2002)

The surface modifications induced by treating $Cu(In,Ga)(S,Se)_2$ films in an aqueous ammonia hydroxide-based solution of Cd^{2+} ions—as used in record $Cu(In,Ga)(S,Se)_2$ solar cells without a CdS buffer layer—have been investigated for different Cd^{2+} concentrations. Employing a combination of x-ray photoelectron spectroscopy, Auger electron spectroscopy, and x-ray emission spectroscopy, it is possible to distinguish two different surface modifications. For Cd^{2+} concentrations below 4.5 mM in the solution we observe the formation of a CdS monolayer, while higher Cd^{2+} concentrations lead to the additional deposition of a cadmium hydroxide film on the $CdS/Cu(In,Ga)(S,Se)_2$ surface. © *2003 American Institute of Physics.*
[DOI: 10.1063/1.1539553]

Today, the standard structure of thin-film solar cells based on $Cu(In,Ga)(S,Se)_2$ (CIGSSe) contains a thin CdS buffer layer (~20 nm) prepared by chemical bath deposition (CBD). Record efficiencies both on a laboratory scale [18.8% (Ref. 1)] and for large-area commercial modules [12.1% for 3651 cm^2 (Ref. 1)] have been achieved with cells containing such a buffer layer. However, one is interested in replacing CdS by a cadmium-free compound or even in fully omitting the buffer layer for waste minimization reasons. One promising route is the deposition of an ''ion layer gas reaction'' (ILGAR) ZnO layer.[2] This layer has been termed the ''window extension layer'' (WEL) (Ref. 2) because the standard window layer itself consists of ZnO (i.e., sputtered *n*-ZnO on top of *i*-ZnO). With this approach, cell efficiencies of 14.6% have been achieved even without the sputtered *i*-ZnO layer, comparable to the corresponding standard structure with a CBD CdS buffer layer (14.7%).[3]

The high efficiencies with WEL layers were made possible by treating the CIGSSe absorber with an ammonium hydroxide solution containing Cd^{2+} prior to the ZnO deposition, which leads to an increase in short circuit current, open circuit voltage, and fill factor.[2] Such a treatment was first proposed for $CuInSe_2$ by Ramanathan and co-workers[4,5] and later successfully employed also by other groups.[6,7] Even though there is still some Cd involved, the total amount in the cell as well as the amount of Cd-containing waste is largely reduced in comparison to the CBD CdS process. The purpose of the treatment is to simulate the beneficial effects of the CBD CdS process, such as a reduction of oxygen surface contaminations,[8] but without the sulfur source (i.e., thiourea). According to a model first proposed by Cahen and Noufi,[9] oxygen passivates the Se deficiencies at grain boundaries and at the surface. While this is expected to have a positive effect at grain boundaries, it leads to a detrimental reduction of the band bending towards the absorber surface, which, in turn, can be reversed by the removal of oxygen (e.g., during the CdS CBD process).[10,11] Furthermore, several groups speculate about a Cd diffusion into the absorber, leading to an *n*-type doping of the absorber surface region.[6,12] Despite its success, the treatment is an ''empirical'' preparation step, and its impact on the absorber surface properties is still largely unknown. In order to gain detailed insight into the chemical and electronic modifications induced by the Cd^{2+} treatment we have, therefore, performed a combined x-ray photoelectron spectroscopy (XPS), x-ray excited Auger electron spectroscopy (XAES), and x-ray emission spectroscopy (XES) study on various modified absorbers.

The investigated CIGSSe absorbers were taken from the Siemens & Shell Solar base-line[13] consisting of a rapid thermal annealing of elemental layers on Mo-coated soda-lime glass in a sulfur-containing atmosphere. Secondary ion mass spectroscopy profiles and XPS experiments show that the Ga content at the absorber surface is negligible and that, hence, our experiments apply to Ga-free $CuIn(S,Se)_2$ (CISSe). To study the concentration dependence, we used Cd^{2+} solutions containing between 0 and 12 mM $CdSO_4$ dissolved in 1.5 M aqueous NH_3. The absorbers were treated for 10 min while employing a temperature ramp between room temperature and 80 °C.[3,5] For XPS and XAES experiments, Mg $K\alpha$ excitation and a VG CLAM 4 electron spectrometer were used. The XES spectra were taken at the SXF endstation of beamline 8.0 at the Advanced Light Source, Berkeley, CA.

In our XPS survey spectra (not shown) we observe a removal of Na after all Cd^{2+} treatments. Furthermore, a re-

[a]Electronic mail: heske@physik.uni-wuerzburg.de

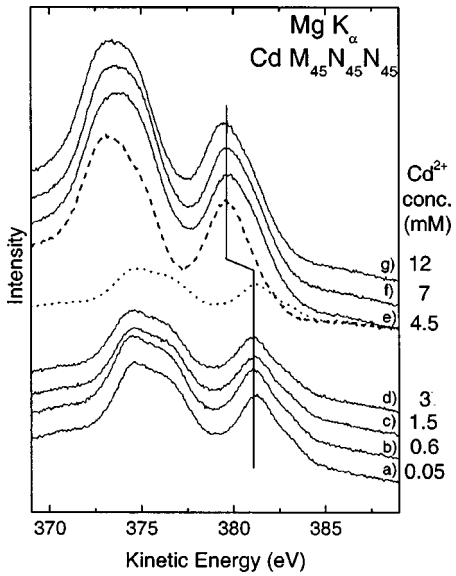

FIG. 1. Cd $M_{45}N_{45}N_{45}$ Auger spectra of $Cu(In,Ga)(S,Se)_2$ absorbers after treatment with different Cd^{2+} concentrations [0.05–12 mM, spectra (a)–(g)], revealing two different Cd species in the different concentration regimes. As an example, the dashed and dotted curves indicate the two contributions to spectrum (e).

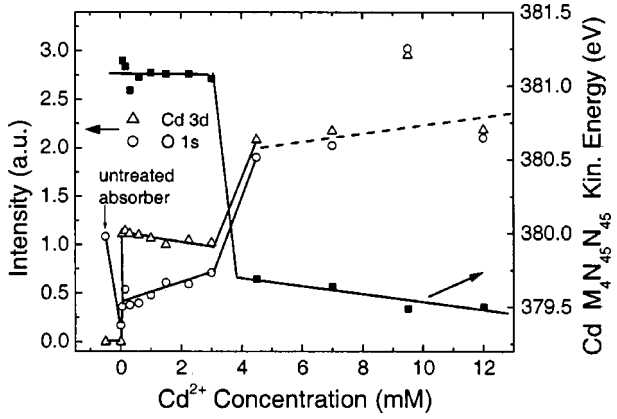

FIG. 2. XPS intensities of Cd 3*d* (open triangles) and O 1*s* (open circles) before and after Cd^{2+} treatment of a $Cu(In,Ga)(S,Se)_2$ absorber (left ordinate). The corresponding Cd $M_4N_{45}N_{45}$ Auger line positions are shown with filled squares (right ordinate).

duction of the native O content at the absorber surface can be observed when using $CdSO_4$ concentrations up to 3 mM, while concentrations of 4.5 mM and above lead to an *enhancement* of the O signal. After all treatments containing Cd^{2+} ions, Cd is detected on the CISSe surface. In contrast to Ramanathan *et al.*[5] and Wada *et al.*,[6] who propose a Cd diffusion *into* the absorber film, we observe a deposition of a Cd-containing layer *on* the absorber surface, as indicated by the attenuation of the substrate XPS and AES peaks. As a function of concentration this deposition takes place in two different regimes, as shown in Fig. 1 for the Cd $M_{45}N_{45}N_{45}$ Auger emission line. Up to a concentration of 3 mM the Auger peak intensity and position is relatively constant, while for higher concentrations, we observe a shift of the Cd *MNN* to lower kinetic energies by 1.5 eV, in parallel with a strong increase in peak intensity. The dashed and dotted lines in Fig. 1 represent a data analysis of the 4.5 mM spectrum to reveal two different Cd species and will be discussed below.

The peak positions of Fig. 1 are summarized in Fig. 2, where, in addition, the corresponding O 1*s* and Cd 3*d* XPS intensities are shown. Already for the lowest used concentration (0.05 mM), a significant Cd concentration at the absorber surface is detected, which decreases slightly with increasing concentrations up to 3 mM. In parallel, we observe a slightly increasing O signal. This behavior of the O content can be understood as a competitive interaction between surface etching by the NH_3 solution and film deposition of Cd-containing species. Assuming that higher Cd^{2+} concentrations lead to an enhanced deposition speed of the Cd layer, the increasing O 1*s* intensity for higher concentrations can then be understood by a diminished etching time of the absorber surface. Based on the absorber peak attenuation and Cd peak intensities, the Cd amount of this layer can be estimated to be between 0.5 and 1 Cd monolayer.

For $CdSO_4$ concentrations of 4.5 mM and above, we find a step in the O 1*s* intensity, in parallel to a step in the Cd 3*d* XPS intensity and a shift of the Cd $M_4N_{45}N_{45}$ Auger line position. The Auger parameter, here defined as the sum of the binding energy of the Cd $3d_{5/2}$ level and the kinetic energy of the main feature of the Cd $M_4N_{45}N_{45}$ transition, shifts from 786.4 to 785.1 eV. The latter value suggests the formation of $Cd(OH)_2$ (Ref. 14) in the high-concentration regime, in accordance with the increase of the O 1*s* intensity, and the molecular-like shape of the O *KVV* Auger line (not shown) resembling that of other hydroxides.[15]

Apart from the shift of the Cd MNN Auger lines for higher Cd^{2+} concentration, a broadening of the spectral features can be observed. In general, the Cd MNN line shapes are very similar for different chemical species because of the localized character of the core hole decay. Hence, this broadening is attributed to a second chemical species in addition to the $Cd(OH)_2$, namely, the same species as observed for lower Cd^{2+} concentrations. To illustrate this assignment we have subtracted an arbitrary fraction (50%) of spectrum (a) in Fig. 1 (dotted line) from spectrum (e) to ''restore'' the characteristic Cd MNN line shape (dashed line). While XPS and XAES give strong evidence for an additional $Cd(OH)_2$ deposition in the high concentration regime, the identification of the species formed at low concentrations is more difficult. XPS and XAES line positions and Auger parameters point towards CdS and/or CdSe, which are not easily distinguished. To do this, we have performed XES experiments for an untreated and a Cd^{2+}-treated (1.5 mM $CdSO_4$) absorber, which give detailed information about the local chemical bonding of the sulfur atoms, as shown in the S $L_{2,3}$ XES spectra in Fig. 3. A detailed discussion of the different features included in this spectrum can be found in Refs. 16 and 17. XES, as a ''photon-in–photon-out'' technique, is much less surface sensitive than XPS or XAES. In our case, the main part of the XES spectrum is associated with the upper 100–200 nm of the CIGSSe film. To get information about the changes induced by the Cd^{2+} treatment at the absorber surface we have subtracted the spectrum of the untreated absorber (a) from that of the Cd^{2+}-treated film (b) (both normalized to maximum count rate) in Fig. 3, yielding spectrum (c). A comparison with a reference spectrum of CdS [Fig. 3(e), see, also, Ref. 18] suggests the formation of CdS at the absorber surface, particularly by noting

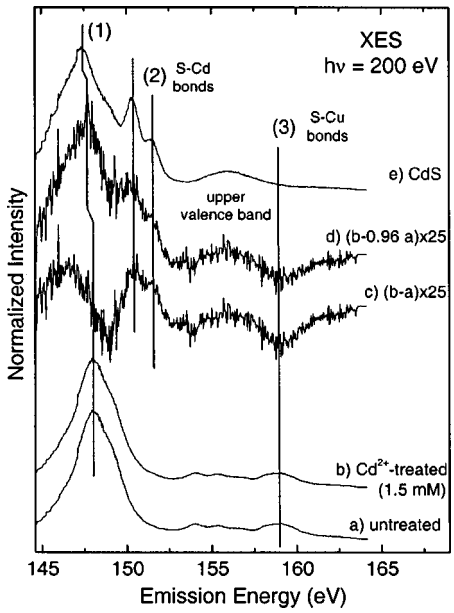

FIG. 3. Sulfur $L_{2,3}$ x-ray emission spectra of (a) an untreated and (b) a Cd^{2+}-treated $Cu(In,Ga)(S,Se)_2$ absorber (1.5 mM Cd^{2+} concentration) normalized to maximum count rate. Spectrum (c) shows the enlarged ($\times 25$) difference of (a) and (b). The spectral features at lines (2) indicate the formation of CdS, which is corroborated by spectrum (d) obtained by subtracting 96% of spectrum (a) from spectrum (b). For comparison, spectrum (e) was taken for a CdS-reference film.

the two peaks at 150.4 and 151.5 eV (marked by vertical lines 2). These peaks correspond to Cd $4d$ electrons decaying into the S $2p_{1/2}$ and $2p_{3/2}$ core holes, respectively, and appear only for sulfur atoms bound directly to Cd. Additionally, we observe the upper valence band of CdS at about 156 eV. Consequently, for spectrum (d), we have subtracted a suitable amount (96%) of spectrum (a) from (b). This subtraction assumes that 4% of the sulfur signal stems from atoms in S–Cd bonds, while 96% of the signal is due to S atoms in the CIGSSe environment. The derived difference spectrum (d) very closely resembles the CdS reference spectrum with the exception of the ''dip'' at 159 eV, to be discussed below. In particular, we now observe the S $3s$-derived main line (1), the Cd $4d$-derived peaks (2), and the upper valence band of CdS. The assumed 4% of CdS signal intensity corresponds to approximately 1 ML of CdS, in agreement with the layer thickness determined from XPS and XAES substrate signal attenuation, as discussed above. The shift of the S $3s$-derived main line (1) is associated with a chemical shift of the S $2p$ core holes, which is also observed in the S $2p$ spectra as a line broadening (not shown).

We now turn to the question of the origin of the sulfur atoms forming the CdS layer. As mentioned above, a dip at about 159 eV (line 3) is observed in spectrum (c). This spectral region is associated with Cu $3d$-derived states and, hence, directly probes S–Cu bonds.[16] In the present case, the Cd^{2+} treatment apparently breaks some of these bonds. This is in accordance with the chemical picture that the S atoms for the CdS formation stem from the absorber surface because the SO_4^{2-} dissolved in the bath is chemically very stable.

In summary, we can derive the following picture of the Cd^{2+} treatment process. For concentrations up to 3 mM we observe the formation of a thin ($\sim$1 ML) CdS film, largely independent of the Cd^{2+} concentration. The S atoms used for the CdS formation stem from the absorber surface, as evidenced by the breakup of S–Cu bonds. Without additional diffusion processes,[18] the CdS deposition is limited to about 1 ML, i.e., to a state in which all S surface atoms are bound to Cd atoms, as corroborated by the intensity behavior of XPS and XAES signals. For concentrations of 4.5 mM and above (at constant concentration of the complexing NH_3) we find an additional $Cd(OH)_2$ layer on top of the CdS layer. Since record CdS-free CISSe solar cells are generally prepared in the low concentration regime, it is evidently the influence of the CdS/CISSe interface formation that is responsible for the empirical success of the Cd^{2+} treatment. In particular, the positive impact of the CdS/CISSe interface on the electronic structure[19,20] is expected to play an important role in the optimization of next-generation, nominally CdS-free thin-film solar cells on the basis of CISSe.

The authors gratefully acknowledge the technical support of the ALS staff, as well as funding by the German BMBF (project FKZ 0329218C) and the Deutsche Forschungsgemeinschaft through SFB 410, TP B3.

[1] M. A. Green, K. Emery, D. L. King, S. Igari, and W. Warta, Solar Cell Efficiency Tables (Version 17); Prog. Photovoltaics **9**, 49 (2001).
[2] M. Bär, H.-J. Muffler, Ch.-H. Fischer, S. Zweigart, F. Karg, and M. C. Lux-Steiner, Prog. Photovoltaics **10**, 173 (2002).
[3] M. Bär, Ch.-H. Fischer, H.-J. Muffler, S. Zweigart, F. Karg, and M. C. Lux-Steiner, Sol. Energy Mater. Sol. Cells **75**, 101 (2002).
[4] K. Ramanathan, R. N. Bhattacharya, J. Granata, J. Webb, D. Niles, M. A. Contreras, H. Wiesner, F. S. Hasoon, and R. Noufi, Proceedings of the 26th PVSC, Anaheim (1997), p. 319.
[5] K. Ramanathan, H. Wiesner, S. Asher, D. Niles, R. N. Bhattacharya, J. Keane, M. A. Contreras, and R. Noufi, Proceedings of the 2nd World Conference of Photovoltaic Energy Conversion, Vienna (1998), p. 477.
[6] T. Wada, S. Hayashi, Y. Hashimoto, S. Nishiwaki, T. Sato, T. Negami, and M. Nishitani, Proceedings of the 2nd World Conference of Photovoltaic Energy Conversion, Vienna (1998), p. 403.
[7] B. Canava, J.-F. Guillemoles, E.-B. Yousfi, P. Cowache, H. Kerber, A. Loeffl, H.-W. Schock, M. Powalla, D. Hariskos, and D. Lincot, Thin Solid Films **361-362**, 187 (2000).
[8] A. Kylner, J. Electrochem. Soc. **146**, 1816 (1999).
[9] D. Cahen and R. Noufi, Appl. Phys. Lett. **54**, 558 (1989).
[10] L. Kronik, U. Rau, J.-F. Guillemoles, D. Braunger, H.-W. Schock, and D. Cahen, Thin Solid Films **361-362**, 353 (2000).
[11] U. Rau, D. Braunger, R. Herberholz, and H.-W. Schock, J. Appl. Phys. **86**, 497 (1999).
[12] T. Nakada and A. Kunioka, Appl. Phys. Lett. **74**, 2444 (1999).
[13] V. Probst, W. Stetter, W. Riedl, H. Vogt, M. Wendl, H. Calwer, S. Zweigart, K.-D. Ufert, B. Freienstein, H. Cerva, and F. H. Karg, Thin Solid Films **387**, 262 (2001).
[14] C. D. Wagner, in *Practical Surface Analysis*, edited by D. Briggs and M. P. Seah (Wiley, New York, 1990), Vol. 1, p. 595.
[15] J. C. Fuggle, E. Umbach, R. Kakoschke, and D. Menzel, J. Electron Spectrosc. Relat. Phenom. **26**, 111 (1982).
[16] C. Heske, U. Groh, O. Fuchs, E. Umbach, N. Franco, C. Bostedt, L. J. Terminello, R. C. C. Perera, K. H. Hallmeier, A. Preobrajenski, R. Szargan, S. Zweigart, W. Riedl, and F. Karg, Phys. Status Solidi A **187**, 13 (2001).
[17] C. Heske, U. Groh, L. Weinhardt, O. Fuchs, B. Holder, E. Umbach, C. Bostedt, L. J. Terminello, S. Zweigart, T. P. Niesen, and F. Karg, Appl. Phys. Lett. **81**, 4550 (2002).
[18] C. Heske, D. Eich, R. Fink, E. Umbach, T. van Buuren, C. Bostedt, L. J. Terminello, S. Sakar, M. M. Grush, T. A. Callcott, F. J. Himpsel, D. L. Ederer, R. C. C. Perera, W. Riedl, and F. Karg, Appl. Phys. Lett. **74**, 1451 (1999).
[19] M. Morkel, L. Weinhardt, B. Lohmüller, C. Heske, E. Umbach, W. Riedl, S. Zweigart, and F. Karg, Appl. Phys. Lett. **79**, 4482 (2001).
[20] L. Weinhardt, M. Morkel, Th. Gleim, S. Zweigart, T. P. Niesen, F. Karg, C. Heske, and E. Umbach, Proceedings of the 17th EPSEC (2002), p. 1261.